Electronic Supplementary Material (ESI) for Nanoscale.

Supporting Information

The cubic to hexagonal phase transition of cerium oxide particles: dynamics and structure

Jan Höcker, Jon-Olaf Krisponeit, Thomas Schmidt, Jens Falta
and Jan Ingo Flege

April 21, 2017

Reciprocal lattice map

Fig. S1 shows a reciprocal lattice map calculated from the bulk lattice parameters of cerium oxide[1] and ruthenium[2]. c-Ce_2O_3 and a-Ce_2O_3 can be clearly distinguished due to the different reflection positions in l-direction. Due to the strong similarity of the in-plane lattice constants of the different cerium oxide crystallographic phases (resulting in very similar k-values), the marked cut through reciprocal space enables an efficient detection of the various components. On Ru(0001), the cubic phases CeO_2 and c-Ce_2O_3(111) appear with rotational domains of 180 °. For clarity, only reflections of one domain are shown in the reciprocal lattice map. However, the positions of these omitted reflections can be easily constructed by mirroring the ceria reflections found in the negative k half space to the positive half space of the map.

Initial reduction from CeO_2(111) to c-Ce_2O_3(111)

The initial reduction from CeO_2 to c-Ce_2O_3 was monitored by $I(V)$-LEEM. As known from previous studies, the reduction of CeO_2 to Ce_2O_3 proceeds by the formation of domains of ordered oxygen vacancies adopting superstructures of $(2 \times 2) \rightarrow (3 \times 3) \rightarrow (4 \times 4)$, where the (4×4) superstructure is associated with c-Ce_2O_3(111).[3,4] In order to estimate the oxidation state of the cerium oxide during thermal reduction, the $I(V)$ curves were directly fitted by a linear combination of the raw (unprocessed) $I(V)$ reference curves of CeO_2(111), $I_0(V)$, and c-Ce_2O_3(111), $I_1(V)$, (cf. Fig. S2a):

$$I(V) = a_0 I_0(V) + a_1 I_1(V).$$

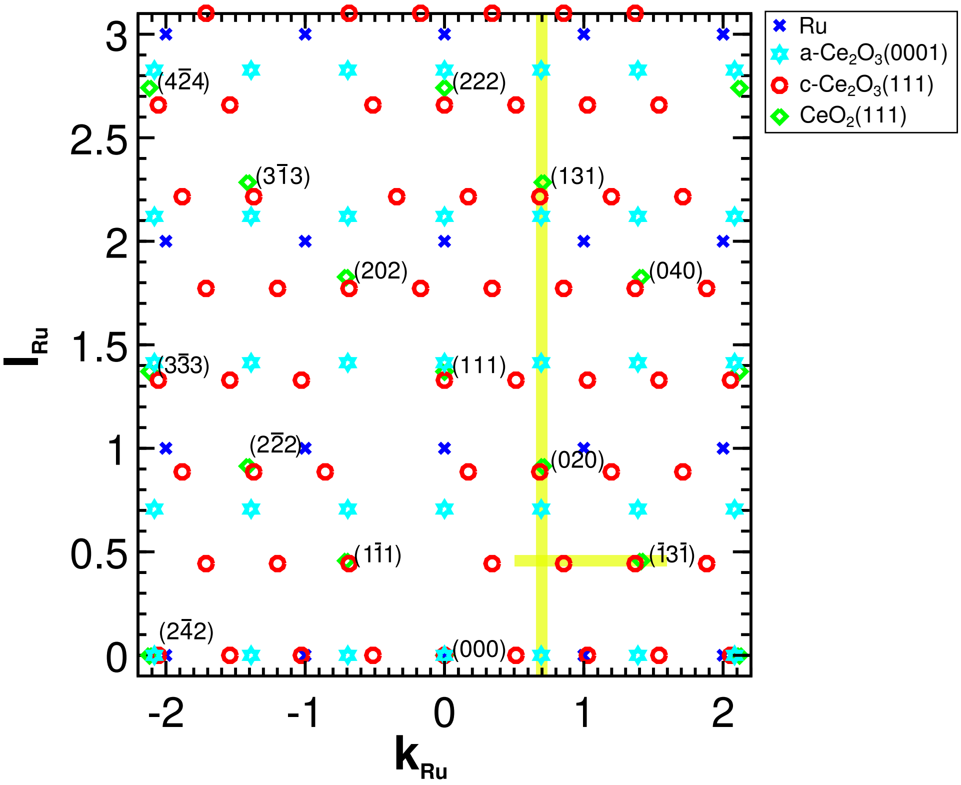

Figure S1: Reciprocal lattice map illustrating the positions of the reflections of the different cerium oxide crystallographic phases as well as of the Ru(0001) substrate. The reflections of CeO_2(111) are labeled by their bulk coordinates. The yellow line highlights the crystal truncation rods discussed in the paper.

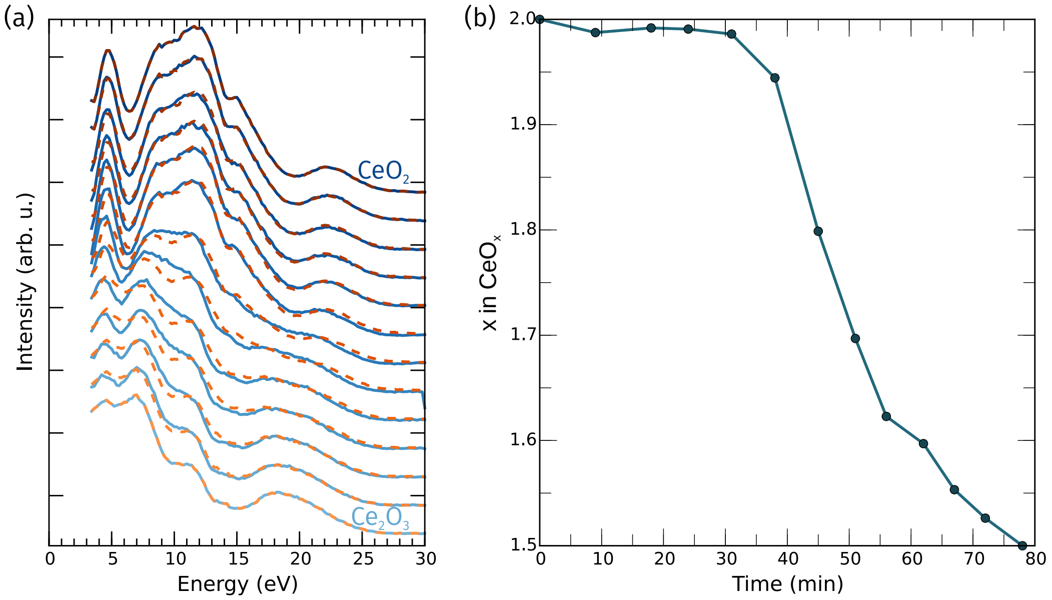

Figure S2: (a) I(V) curve sequence acquired during thermal reduction at 700 °C (full lines) and fit by a linear combination of the I(V) curves of $CeO_2(111)$ and of c-$Ce_2O_3(111)$ (dashed lines). (b) Cerium oxide oxidation state during thermal reduction calculated from the coefficients obtained by the fit in (a).

The stoichiometry CeO_x was then calculated from the coefficients as follows:

$$x = \frac{a_0}{a_0 + a_1} \cdot 0.5 + 1.5.$$

This procedure cannot be expected to fully reproduce the $I(V)$ curves recorded from the ceria especially in an intermediate stoichiometry of $CeO_{1.8}$ to $CeO_{1.7}$ since the $I(V)$ curve resulting from the linear combination cannot include structure-specific spectral elements of, e. g., the (3 × 3) superstructure,[4] but only spectral features that are already part of the two reference curves for $CeO_2(111)$ and c-$Ce_2O_3(111)$. However, this approach readily provides an estimate of the cerium oxide stoichiometry changing with heating time as plotted in Fig. S2b. Accordingly, it takes up to 30 min until a notable reduction is observable by $I(V)$-LEEM. Most probably, a certain degree of reduction has occurred in this time frame already, but as long as the oxygen vacancies remain relatively scarce and statistically disordered, the unoccupied band structure is largely unaffected, hence making this amount of reduction essentially invisible to $I(V)$-LEEM. Subsequently, the rate of reduction is seen to increase until a stoichiometry of $CeO_{1.6}$ is reached. Afterwards, the reduction speed slows down slightly until after 80 min the cerium oxide is fully reduced to c-$Ce_2O_3(111)$.

Phase transition from c-Ce_2O_3(111) to a-Ce_2O_3(0001)

The supplemental video S1 shows the phase transition from c-Ce_2O_3 to a-Ce_2O_3(0001) at 700 °C. As this movie is part of a dynamic $I(V)$-LEEM experiment, please note that the electron kinetic energy is set to values from 3 eV to 30 eV in 0.2 eV steps; thus energy-dependent changes in image contrast are observed in addition to the contrast changes reflecting alterations in the structure and morphology of the sample.

References

[1] G. Adachi and N. Imanaka, *Chem. Rev.*, 1998, **98**, 1479–1514.

[2] J. W. Arblaster, *Platinum Metals Rev.*, 2013, **57**, 127–136.

[3] V. Stetsovych, F. Pagliuca, F. Dvořák, T. Duchoň, M. Vorokhta, M. Aulická, J. Lachnitt, S. Schernich, I. Matolínová, K. Veltruská, T. Skála, D. Mazur, J. Mysliveček, J. Libuda and V. Matolín, *J. Phys. Chem. Lett.*, 2013, **4**, 866–871.

[4] J. Höcker, T. O. Menteş, A. Sala, A. Locatelli, T. Schmidt, J. Falta, S. D. Senanayake and J. I. Flege, *Adv. Mater. Interf.*, 2015, **2**, 1500314.